

Characterization of copper oxidation by linear potential sweep voltammetry and UV-Visible-NIR diffuse reflectance spectroscopy

M. LENGLET, K. KARTOUNI, D. DELAHAYE

Laboratoire de Physicochimie des Matériaux, INSA-Université de Rouen, BP 08, 76131 Mont-Saint-Aignan Cedex, France

Received 13 December 1990; revised 12 February 1991

The aim of this study was to characterize the compounds grown on copper during oxidation at low temperature ($T < 573$ K) in air by electrochemical and optical methods. The following oxides have been characterized: a precursor Cu_xO of mixed valency character, a non stoichiometric cuprous oxide, CuO and its precursor. The mechanism of reduction has been established for layers containing CuO and a non stoichiometric copper(I) oxide. CuO is reduced before cuprous oxide. In complicated cases, it is impossible to draw conclusions from the characteristics of the electrochemical reduction (the first step of CuO reduction and the reduction of Cu(I) species specific of the non-stoichiometry are observed at the same potential). Nevertheless, the association of a non-destructive technique such as diffuse reflectance spectroscopy and electrochemical methods allows identification of the different species present in corrosion layers on copper surfaces.

1. Introduction

Previous studies have shown that low temperature oxidation ($T < 573$ K) of copper films [1] on bulk copper [2], [3] leads to the formation of a phase Cu_3O_2 before that of CuO , which is the only thermodynamically stable phase. Cu_3O_2 is a gross defect structure of Cu_2O . Stoichiometric Cu_2O cannot be obtained in these experimental conditions during oxidation of bulk copper.

The characterization of oxidation products, developed on copper during thermal treatments can be carried out by different methods:

- with physical methods, like XPS, SIMS and electron microprobe when the sample must be examined under ultra high vacuum;
- with optical methods, like u.v.-vis.-n.i.r. diffuse reflectance spectroscopy, FTIR and photoluminescence spectroscopies, when the samples can be studied without any special preparation; and
- with electrochemical methods, such as linear potential sweep voltammetry, and coulometry which allow the identification of copper(I) and copper(II) oxides.

In this paper we present linear potential sweep voltammetric studies of the reduction of copper oxides grown on copper during low temperature thermal treatment correlated with the analysis of diffuse reflectance spectra in the 200–2500 nm range.

2. Experimental details

Circular copper electrodes, 0.5 mm thick with 1.13 cm² surface area were used. The specimens were either

etched in nitric acid or mechanically polished, rinsed in absolute ethanol before thermal oxidation at the appropriate temperature. The chemical compositions of the industrial metals from which specimens were cut were as indicated in Table 1.

The three following electrolytes were used: 0.1 M $\text{Na}_2\text{B}_4\text{O}_7$, 0.1 M NaCH_3COO (at pH ~ 9 ; the solubility of the different copper compounds, oxides and hydroxides is minimum) and 0.1 M NaCl . The electrochemical reduction curves were determined using a sample holder, an electrochemical cell fitted with a platinum counter electrode and a saturated calomel electrode (SCE) as reference. Before each run the electrolyte was carefully purged with nitrogen. The reduction speed was 0.5 mV s^{-1} . The u.v.-vis.-n.i.r. diffuse reflectance spectra were performed on a Perkin Elmer Lambda 9 spectrophotometer equipped with an integrating sphere (BaSO_4).

3. Analysis of oxide films by diffuse reflectance spectroscopy

3.1. Precursor Cu_xO

The oxidation process of copper begins with the growth of a precursor Cu_xO having the same crystallographic structure as Cu_2O but with different XPS and u.v. spectra [4]. In the initial stages of copper oxidation, the same u.v.-vis. diffuse reflectance spectrum is observed for all kinds of copper (ETP, OFHC and DHP) whatever the temperature of oxidation. These spectra are close to that of metallic copper except for an absorption band in the 360–380 nm range and the shift of the maximum absorption from

Table 1.

Impurity (p.p.m.)	O	Ag	As	Pb	Fe	Ni	Sb	S	Se	Te
ETP copper (for copper a, according to French nomenclature)	100	≤ 10	≤ 10	≤ 10	≤ 10	≤ 10	≤ 5	≤ 5		≤ 5
OFHC copper (for copper c, according to French nomenclature)	31	6	2	2	1	2	6		1	1

285 to 300 nm (curve a Fig. 1). From atom probe, XPS and Auger studies [4], one can conclude that the precursor Cu_xO has a mixed valency character containing interstitial Cu^0 scattered in the Cu(I) oxide phase and corresponds to a diffuse interface of approximately 10–15 nm (the oxygen and copper concentration profiles vary continuously from surface to bulk copper).

3.2. Non stoichiometric cuprous oxide

The u.v.-vis.-n.i.r. spectra of cuprous oxide grown on copper (at high or low temperature) exhibit bands between 400 and 550 nm (Fig. 1, curve b).

These bands, not observed in the case of stoichiometric Cu_2O (Table 2), are due to electronic defects in the cuprous oxide.

The superficial layer of copper(I) oxide, formed by oxidation of ETP copper in air at 573 K (annealing time 5 min) was analysed by electron microprobe. The average atomic concentration of oxygen and copper (excitation energy: 6 kV) corresponds to the $\text{Cu}_{61}\text{O}_{39}$

formula [3]. A model based on that of Tolstoi [11] has been developed by Machefer [12] in order to explain the influence of electronic defects on the optical spectrum of cuprous oxide. The calculation with the oft-quoted experimental gap value of 2.2 eV leads to an absorption band at 510 nm for copper vacancies and another at 670 nm for oxygen vacancies.

The electronic defects can be more precisely identified on photoluminescence spectra of samples oxidized at high temperature (~ 1273 – 1323 K). It has been established that the luminescence spectrum of Cu_2O crystals contains three bands at 0.72, 0.82 and 0.93 μm . The short-wave bands are attributed to oxygen vacancies and the i.r. band at 0.93 μm to copper vacancies. In all the important features the spectra measured in thin Cu_2O films (1.0 to 3.0 μm) [13] are identical to those measured in thicker films [14] to [16] or in crystals at the same temperature. Studies of Cu_2O excitation at 77 K have shown that the relaxed exciton emissions at oxygen and copper vacancies are readily observable for all wavelengths from 630 to 400 nm. The excitation spectra for the 920 nm copper vacancy emission reveal three components at 480, 540 and 590 nm (intensity maximum at 480 nm).

Wieder and Czanderna [17] have studied the optical properties of $\text{CuO}_{0.67}$ (or Cu_3O_2) thin films obtained by low temperature oxidation of copper films. From the transmittance and reflectance measurements in the wavelength region of 400 to 800 nm these authors deduced the wavelength dependence of the optical constants (refractive index and absorption coefficient). The appearance of the dispersion peak in the index of refraction curve of $\text{CuO}_{0.67}$ at about 2.34 eV is characteristic of the presence of an absorption edge at that energy (in agreement with the 2.3 eV value for the gap width, at room temperature). The absorption curve of this oxide is characterized by the absence of a peak in the range 400–550 nm and by a very strong unexplained absorption below the band gap. At 400 nm, the absorption coefficient of $\text{CuO}_{0.67}$ is stronger by one order of magnitude than that of bulk Cu_2O .

Jaenicke *et al.* [2] have observed Cu_3O_2 during oxidation of either Cu_2O or Cu. The range of stability of Cu_3O_2 is greater than found previously.

3.3. CuO

The optical spectrum for cupric oxide is characterized by an abrupt rise in absorption in the range 800–

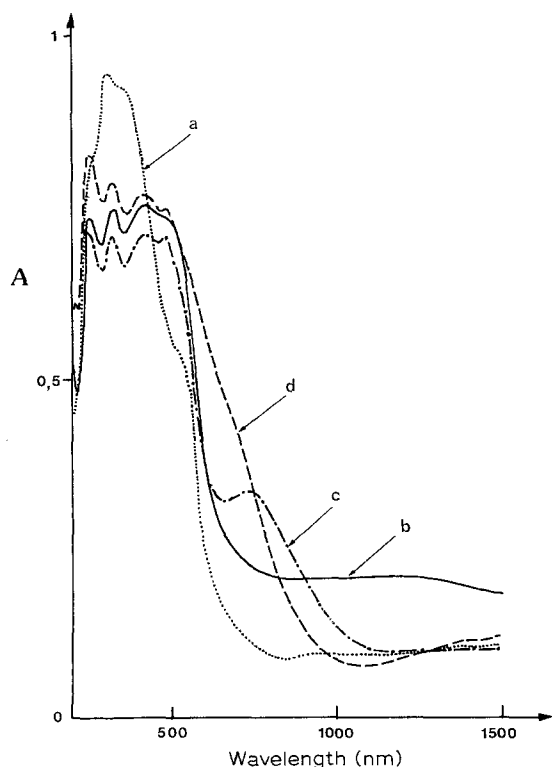


Fig. 1. Optical spectrum of copper oxidized in air at 523 K: curve (a) 2, (b) 10, (c) 30 and (d) 60 min.

Table 2. Theoretical and experimental data relative to optical spectra of cuprous oxide.

Samples	Transition energy (eV)					Ref.
	A	$E_1\beta$	E_2	E_3	C	
Cu ₂ O stoichiometric	Experimental	3.33	4.30	4.75	5.50	[5]
		3.60	4.30–4.50	4.70	4.90	5.60 (at 77 K)
	Theoretical	3.30	4.0–4.40	4.70	5.10	[7]
		3.79	4.03	4.55	4.94	5.20
Cu ₂ O non-stoichiometric (high temp.)	2.34 (530)	3.09 (400)	3.77	4.5–4.95	(at 77 K)	this study
Cuprous oxide	2.25–2.58	2.82–2.95	3.75–3.80	4.75–4.95		[9], [10] and this study
Cu _x O _y (low temp.)	(550–480)	(440–420)	(330–325)	(260–250)		

360 major peaks (530) wavelength in nm

900 nm. No other salient features are observed up to 200 nm. The u.v.-vis.-n.i.r. spectrum of the 3d⁹ Jahn–Teller in an octahedral environment is well known and consists of three transitions: $0_1^2B_{1g} \rightarrow ^2A_{1g}$, $0_2^2B_{1g} \rightarrow ^2B_{2g}$, $0_3^2B_{1g} \rightarrow ^2E_g$ in the range 600–1300 nm (for MgO: Cu²⁺, two bands are observed at about 9500 and 11230 cm⁻¹ [18]). The broad absorption observed for CuO is due to the complex magnetic structure and to a large overlapping between d-d transitions and charge transfer bands. The curve d on Fig. 1 reveals the presence of CuO on a non-stoichiometric cuprous oxide film.

4. Study of the electrochemical reduction curves

Several investigators have recognized that techniques based on electrochemical reduction can be useful for characterizing oxide layers on copper [19] to [23]. Deutscher and Woods [23] have shown that both copper oxides Cu₂O and CuO could be distinguished from the potentials of their cathodic reduction peaks and concluded from their experimental results that the Pops and Hennessy [2] galvanostatic method for determining oxides formed on copper in the wire industry is very doubtful. Guinement [22] has studied copper contamination in air containing different pollutants and assigned the first peak on the voltammogram to the reduction of Cu₂O and the second to the reduction of CuO. This controversy led us to study the electrochemical reduction of copper oxides formed during low-temperature oxidation using linear potential sweep voltammetry.

4.1. Correlation between spectrophotometric and electrochemical analysis

Figure 2 shows voltammograms obtained for samples oxidized at 523 K (the diffuse reflectance spectra are analysed in § 2). A brief analysis of experimental data is summarized in Table 3.

In all voltammograms, the first minor peak near -0.5 V/SCE is attributable to an oxide similar to the

precursor Cu_xO and the major peak in the range -0.75–0.85 V to the reduction reaction $Cu^+ + e \rightarrow Cu$ in the non-stoichiometric cuprous oxide. In Fig. 2d and 2c, the peak at -0.65 V can be assigned respectively to the first step reduction of CuO or to that of a precursor of CuO [24] (the reduction of CuO powder on a copper substrate is characterized by two unresolved peaks at -0.67 and -0.85 V/SCE [11]).

In order to prove these conclusions, we have investigated the optical spectrum of two samples oxidized at 573 K and reduced progressively in the electrochemical cell.

The first sample was etched in nitric acid and rinsed in absolute ethanol before thermal oxidation (573 K, 60 min). The oxide layer consisted of a thin outer cupric oxide film on an inner non stoichiometric copper(I) oxide layer (Fig. 3a). The spectrum of the sample reduced up to -0.75 V (Fig. 3b) shows a sig-

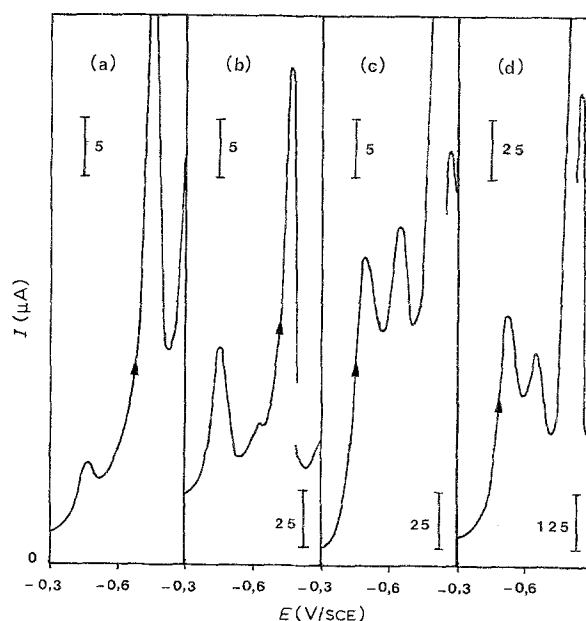


Fig. 2. Potential scans at 0.5 mV s⁻¹ in 0.1 M borax for the reduction of oxides grown on copper at 523 K in air during different times: (a) 2, (b) 10, (c) 30 and (d) 60 min.

Table 3. Analysis of OFHC copper oxidation at 523 K

Samples annealed at 523 K during:	2 mn	10 mn	30 mn	60 mn
Nature of oxide from spectrophotometric analysis	Precursor	n.s. cuprous oxide	n.s. cuprous oxide	n.s. cuprous oxide + CuO
Film thickness (nm) (by coulometric study)	20	130	250	400
Peak position on voltammograms (V/SCE)	-0.47; -0.77	-0.47; -0.77	-0.50; -0.65; -0.87	-0.50; -0.65; -0.85

n.s.: non-stoichiometric.

nificant decrease of the absorption in the range 600–850 nm due to the first step of the reduction of CuO; the spectrum of the non stoichiometric cuprous oxide is unchanged. If the reduction is extended up to -0.80 V, the spectrum reveals the absence of cupric oxide and a slight decrease of the bands in the range 400–500 nm relative to the non-stoichiometry of copper(I) oxide. So, the reduction of CuO is achieved and that of cuprous oxide starts.

Similar results were obtained for the second sample mechanically polished before the oxidizing treatment (573 K, 30 min), but this approach allowed the determination of the thickness by optical interferometry. The results show that CuO is reduced before the copper(I) oxide, in the range -0.70 – 0.80 V.

The reduction of cuprous oxide becomes really effective for more negative potentials (< -0.80 V) as shown by the data in Table 4.

The decrease of absorption near 500 nm (Fig. 4c) suggests that the outer part of the cuprous oxide layer contains more copper vacancies than the middle layer.

In conclusion, the electrochemical reduction of copper oxides in complex layers gives rise to the reactions (Fig. 5).

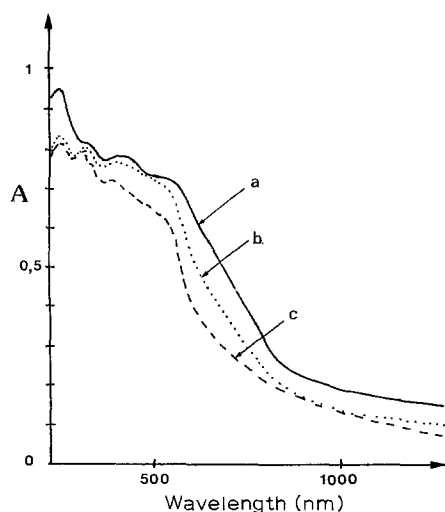
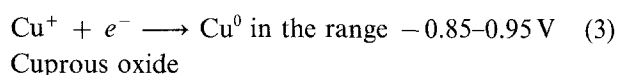
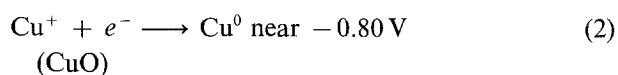
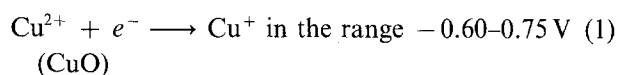


Fig. 3. Optical spectra of an ETP copper sample oxidized in air at 573 K (60 min) before reduction (a) reduced up to -0.75 V (b) and up to -0.80 V (c) in 0.1 M sodium acetate.



An overlapping of Reactions 2 and 3 may be observed (increasing thickness shifts the peak positions to more negative potentials). Our results are in excellent agreement with those of Deutscher and Woods [23] and contradict the conclusions of Pops and Hennessy who mistook CuO for Cu₂O in their study of the reduction of oxide layers formed on copper wires during annealing for 5 s at different temperatures in the range 373–773 K [20].

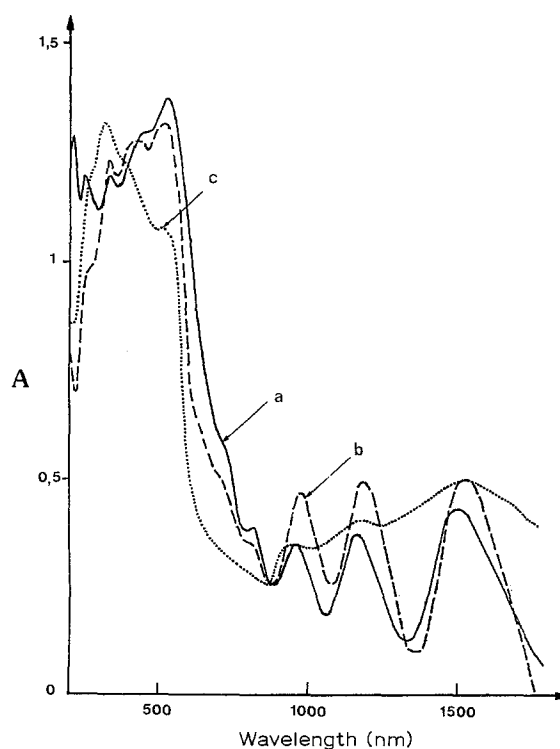


Fig. 4. Optical spectra of an ETP copper sample mechanically polished and oxidized in air at 573 K (30 min) before reduction (a), reduced up to -0.80 V (b) and up to -0.85 V (c) in 0.1 M sodium acetate.

Table 4.

	Initial stage	Sample reduced up to V/(SCE)		
Thickness (μm)	1.045	-0.75	-0.80	-0.85
		1.03	1.05	0.965

4.2. Influence of the electrolyte: analytical applications and limitations of the electrochemical study

The following electrolyte solutions were used for experiments: 0.1 M borax, 0.1 M sodium acetate and 0.1 M NaCl. Investigations were carried out on ETP copper samples (etched or mechanically polished) heated in a furnace held at 573 K. The voltammogram observed for the same heat treated samples are similar in different electrolytes; in borax a small shift (0.05–0.10 V) towards more negative potentials is observed. Fig. 6 presents the reduction scans in borax for mechanically polished samples. The experimental data are listed in Table 5.

Sometimes, the voltammograms present a peak or a shoulder in the range -0.50–0.70 V/SCE (Fig. 6a and 6b) whereas other analytical methods (XRD, XPS or diffuse reflectance spectroscopy) do not indicate the presence of copper(II) species (CuO or its precursor). This may be assigned to a copper(I) oxide less stable than Cu₂O (as the precursor Cu_xO). A similar result was obtained by Deutscher and Woods [23] on the voltammogram of an oxide formed by “electrochemical ageing”: a peak at -0.70 V is observed in addition

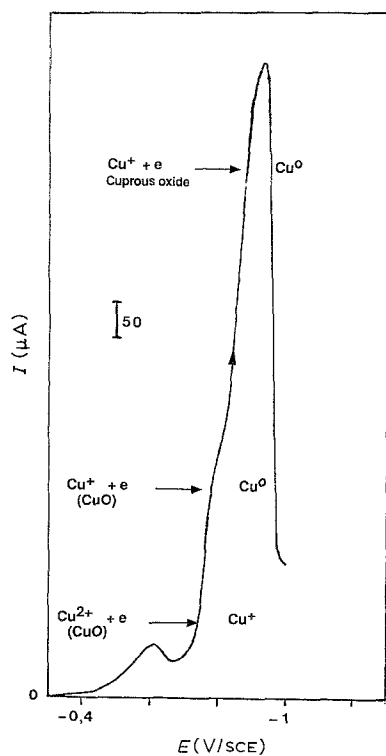


Fig. 5. Evidence of three reduction reactions for an ETP copper sample oxidized at 573 K (15 min).

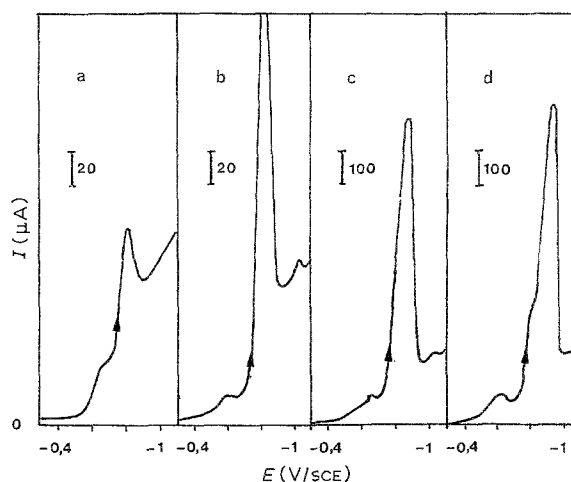


Fig. 6. Electrochemical reduction curves of ETP copper samples oxidized at 573 K (reduction speed: 0.5 mV s⁻¹, 0.1 M Na₂B₄O₇) 2 (a), 4 (b), 10 (c) and 15 min (d).

to the first peak attributable to the precursor. This change in the voltammetric curve is considered by different authors to arise from restructuring of the copper(I) oxide layer, making it more difficult to reduce [23], [25], [26]. Thus, whereas the initial oxide can be reduced close to the reversible potential, a significant overpotential is required to reduce the more stable compounds.

The scan characteristic of the sample 3 (Fig. 6c) reveals three copper oxides: two copper(I) oxides including a non-stoichiometric cuprous oxide (peak at -0.88 V) and a precursor of CuO (identified by an absorption band at 700 nm on the optical spectrum). A similar example is observed in Figs 1c and 2c. The voltammogram of the sample oxidized for 15 min (Fig. 6d) shows unambiguously the two steps due to reduction of CuO (-0.62 and -0.80 V) and the major peak (-0.93 V) attributable to the reduction of the copper(I) oxide.

These experimental data show that the electrochemical method is a valuable technique for the identification of copper oxides in corrosion layers. Nevertheless, in complicated cases, the simultaneous use of a non-destructive method like diffuse reflectance spectrometry, Raman or FTIR spectroscopy is indispensable for unambiguous characterization of different species.

Table 5.

Samples	1	2	3	4
Annealing time (s) at 573 K in air	2	4	10	15
		-0.68 (sh)	-0.61	-0.60 (sh)
				-0.67
Cathodic peak positions (V/SCE)				-0.62
(+Cu ⁺ + e ⁻ → Cu)	-0.80 ⁺	-0.83 ⁺	-0.88 ⁺	-0.80
Cu(I) oxide				-0.93
Thickness* (nm)	40	70	300	350

* From optical measurements; sh: shoulder.

In view of further analytical applications, the electrochemical reduction of thin CuCl films grown on copper has been studied in 0.1 M borax and 0.1 M NaCl. The peaks attributable to the reduction of Cu⁺ in CuCl are respectively observed at -0.58 V and -0.40 V/SCE in these electrolytes. So electrochemical evidence of CuCl in corrosion layers formed on copper by atmospheric contamination requires the use of NaCl as electrolyte for the experiments.

5. Conclusion

The potentials at which copper oxides are reduced vary with oxide thickness and with the non-stoichiometry for cuprous oxides. Nevertheless, the association of a non-destructive technique such as diffuse reflectance spectroscopy and electrochemical methods allows the identification of the different species present in corrosion layers on copper surfaces. The reduction of CuO involves two steps and takes place before that of Cu₂O.

References

- [1] H. Wieder and A. W. Czanderna, *J. Phys. Chem.* **66** (1962) 816.
- [2] H. Neumeister and W. Jaenike, *Z. Phys. Chem.* **B108** (1977) 217.
- [3] M. Lenglet, J. M. Machefert, J. M. Claude, B. Lefez, J. Lopitiaux and A. D'Huysser, *Surf. Interf. Anal.* (1990), in press.
- [4] J. M. Machefert, M. Lenglet, D. Blavette, A. Menand and A. D'Huysser, 'Structure and Reactivity of Surfaces', Elsevier Sciences Publishers B. V., Amsterdam (1989) p. 625.
- [5] M. Balkanski, Y. Petroff and D. Trivich, *Solid. State Commun.* **5** (1967) 85.
- [6] S. Brahms, J. P. Dahl and S. Nikitine, *J. Phys.* (1967) C3-28.
- [7] P. Marksteiner, P. Blaha and K. Schwarz, *Z. Phys.* **B64** (1986) 119.
- [8] W. Y. Ching, Y. N. Xu and K. W. Wong, *Phys. Rev.* **B40** (1989) 7864.
- [9] J. M. Machefert, A. D'Huysser, M. Lenglet, J. Lopitiaux and D. Delahaye, *Mat. Res. Bull.* **23** (1988) 1379.
- [10] M. Lenglet, J. Arsene, J. M. Machefert, P. Leterrable and J. M. Welter, *Analisis* **16** (1988) 2.
- [11] N. A. Tolstoi and V. A. Bonch-Bruevich, *Sov. Phys. Solid State* **13** (1971) 1135.
- [12] J. M. Machefert, Thèse, Rouen (1990).
- [13] B. Lefez and M. Lenglet, unpublished results.
- [14] C. Duvury, D. J. Kenway and F. L. Weichman, *J. Lum.* **10** (1975) 415.
- [15] R. G. Kaufman and R. T. Hawkins, *J. Electrochem. Soc.* **131** (1984) 385.
- [16] R. G. Kaufman and R. T. Hawkins, *J. Electrochem. Soc.* **133** (1986) 2652.
- [17] H. Wieder and A. W. Czanderna, *J. Appl. Phys.* **37** (1966) 184.
- [18] F. H. Chapple and F. S. Stone, *Proc. Brit. Ceram. Soc.* **1** (1964) 45.
- [19] R. H. Lambert and D. J. Trevoy, *J. Electrochem. Soc.* **105** (1958) 18.
- [20] H. Pops and D. R. Hennessy, *Wire J.* **10** (1977) 50.
- [21] H. Strehblow and B. Titze, *Electrochim. Acta* **25** (1980) 839.
- [22] J. Guinement, Thèse Ingénieur Docteur, Paris VI (1985).
- [23] R. L. Deutscher and R. Woods, *J. Appl. Electrochem.* **16** (1986) 413.
- [24] M. O'Keefe and F. S. Stone, *Proc. Roy. Soc.* **A267** (1962) 501.
- [25] M. E. Martins and A. J. Arvia, *J. Electroanal. Chem.* **165** (1984) 135.
- [26] M. R. Gennero de Chialvo, S. L. Marchiano and A. J. Arvia, *J. Appl. Electrochem.* **14** (1984) 165.